A&A 569, L5 (2014)
DOI: 10.1051/0004-6361/201424756

Astronomy & Astrophysics

Letter to the Editor

Revised spectroscopic parameters of SH^+ from ALMA⋆ and IRAM 30 m⋆⋆ observations⋆⋆⋆

Holger S. P. Müller[1], Javier R. Goicoechea[2], José Cernicharo[2], Marcelino Agúndez[2], Jérôme Pety[3,4], Sara Cuadrado[2,5], Maryvonne Gerin[4], Gaëlle Dumas[3], and Edwige Chapillon[3,6,7]

[1] I. Physikalisches Institut, Universität zu Köln, Zülpicher Str. 77, 50937 Köln, Germany
e-mail: hspm@ph1.uni-koeln.de
[2] Instituto de Ciencias de Materiales de Madrid (CSIC), 28049 Cantoblanco, Madrid, Spain.
[3] IRAM, 300 rue de la Piscine, 38406 Saint Martin d'Hères, France
[4] CNRS UMR 8112, LERMA, Observatoire de Paris, École Normale Supérieure and Université Pierre et Marie Curie, 75014 Paris, France
[5] Centro de Astrobiología (CSIC-INTA), Carretera de Ajalvir km 4, 28850 Torrejón de Ardoz, Madrid, Spain
[6] CNRS, LAB, UMR 5804, 33270 Floirac, France
[7] Université de Bordeaux, LAB, UMR 5804, 33270 Floirac, France

Received 5 August 2014 / Accepted 3 September 2014

ABSTRACT

Hydrides represent the first steps of interstellar chemistry. Sulfanylium (SH^+), in particular, is a key tracer of energetic processes. We used ALMA and the IRAM 30 m telescope to search for the lowest frequency rotational lines of SH^+ toward the Orion Bar, the prototypical photo-dissociation region illuminated by a strong UV radiation field. On the basis of previous *Herschel*/HIFI observations of SH^+, we expected to detect emission of the two SH^+ hyperfine structure (HFS) components of the $N_J = 1_0–0_1$ fine structure (FS) component near 346 GHz. While we did not observe any lines at the frequencies predicted from laboratory data, we detected two emission lines, each ∼15 MHz above the SH^+ predictions and with relative intensities and HFS splitting expected for SH^+. The rest frequencies of the two newly detected lines are more compatible with the remainder of the SH^+ laboratory data than the single line measured in the laboratory near 346 GHz and previously attributed to SH^+. Therefore, we assign these new features to the two SH^+ HFS components of the $N_J = 1_0–0_1$ FS component and re-determine its spectroscopic parameters, which will be useful for future observations of SH^+, in particular if its lowest frequency FS components are studied. Our observations demonstrate the suitability of these lines for SH^+ searches at frequencies easily accessible from the ground.

Key words. molecular data – line: identification – ISM: molecules – radio lines: ISM – ISM: individual objects: Orion Bar

1. Introduction

Hydrides, which consist of one heavy atom and one or more H atoms, are of fundamental importance in the interstellar medium (ISM). Unfortunately, their fundamental transitions at submillimeter (sub-mm) wavelengths are often difficult to observe from the ground. The *Herschel* Space Observatory and the Stratospheric Observatory for Infrared Astronomy (SOFIA) have increased our knowledge about hydrides in space considerably. Recent detections include ArH^+ with *Herschel* (Barlow et al. 2013; Schilke et al. 2014) and SH with SOFIA (Neufeld et al. 2012).

The reactive molecular ion SH^+ (sulfanylium) is an interesting probe of energetic processes in the ISM. In particular, SH^+ is only detectable in significant amounts if the very high endothermicity (0.86 eV or ∼9860 K) of the gas-phase reaction

$$S^+ + H_2(v = 0) \rightarrow SH^+(X^3\Sigma^-) + H \quad (1)$$

can be overcome. Using the Atacama Pathfinder EXperiment (APEX) 12 m telescope, Menten et al. (2011) discovered recently sub-mm SH^+ absorption lines in the envelope of the prolific star-forming region Sagittarius B2(M), Sgr B2(M) for short, a very strong continuum source close to the Galactic center, and in the diffuse interstellar clouds on the line of sight toward this source. The ubiquity of SH^+ in diffuse clouds was reemphasized soon thereafter by *Herschel*/HIFI observations toward several Galactic sight lines by Godard et al. (2012). These authors proposed that the required energy for reaction (1) arises from turbulent dissipation, shocks, or shears in these very low density clouds. Sub-mm SH^+ emission lines were also detected by *Herschel* in higher density environments such as the high-mass star-forming region W3 IRS5 (Benz et al. 2010) or the Orion Bar photo-dissociation region (PDR; Nagy et al. 2013). These are strongly UV-irradiated environments where the gas attains high temperatures (≲1000 K) and where H_2 molecules are

⋆ This paper makes use of the following ALMA data: ADS/JAO.ALMA#2012.1.00352.S. ALMA is a partnership of ESO (representing its member states), NSF (USA) and NINS (Japan), together with NRC (Canada) and NSC and ASIAA (Taiwan), in cooperation with the Republic of Chile. The Joint ALMA Observatory is operated by ESO, AUI/NRAO and NAOJ.

⋆⋆ This paper makes use of observations obtained with the IRAM 30 m telescope. IRAM is supported by INSU/CNRS (France), MPG (Germany), and IGN (Spain).

⋆⋆⋆ Appendix A is available in electronic form at http://www.aanda.org

UV-pumped to vibrationally excited states. In addition, in these PDR environments, reaction (1) becomes exothermic when H_2 molecules are in the $v = 2$ or higher vibrational levels, thus enhancing the SH^+ abundance (e.g., Zanchet et al. 2013). Finally, if doubly ionized sulfur atoms co-exist with H_2 molecules in X-ray dissociation regions (XDRs), such as Galactic center clouds (e.g., Godard et al. 2012; Etxaluze et al. 2013), the very exothermic reaction

$$S^{++} + H_2 \rightarrow SH^+ + H^+ + 8.79\ \mathrm{eV} \quad (2)$$

can be a significant source of SH^+ (e.g., Abel et al. 2008).

The strongest ground state FS component of $SH^+(X^3\Sigma^-)$ at ~526 GHz ($N_J = 1_2 - 0_1$) cannot be observed from the ground because of the water in Earth's atmosphere. The ~683 GHz ($N_J = 1_1 - 0_1$) and ~893 GHz ($N_J = 2_1 - 1_1$) transitions can be observed from the ground, albeit with some difficulty. Transitions of the $N_J = 1_0 - 0_1$ FS component at ~346 GHz (Savage et al. 2004) lie in a more accesible frequency window. Indeed, Menten et al. (2011) searched for the SH^+ ~346, ~683, and ~893 GHz absorption lines toward Sgr B2(M). Unfortunately, the ~346 GHz lines are heavily blended with absorption components of the nearby CO $J = 3-2$ line caused by Milky Way spiral arm molecular clouds. Stäuber et al. (2007) detected an emission feature at 345 930 MHz in the massive protostar AFGL 2591, but it may be caused by $^{34}SO_2$, a common species in these sources, so they could not draw firm conclusions about SH^+. Leurini et al. (2006) presented first the results of a 1 mm line survey toward the Orion Bar with the APEX 12 m telescope. They did not report the detection of SH^+. However, they observed the denser HCN clump (Lis & Schilke 2003) and not the most exposed UV-irradiated PDR gas layers where SH^+ is expected.

In this letter we present the first ground-based detection of SH^+ lines toward the Orion Bar CO^+ peak (Stoerzer et al. 1995; Goicoechea et al. 2011, and references therein). We show that the previously reported SH^+ $N_J = 1_0-0_1$ line frequencies at ~346 GHz are not correct and use the frequencies derived from our observations to compute improved SH^+ spectroscopic parameters and line frequencies.

2. Observations

2.1. Single-dish IRAM 30 m observations

IRAM 30 m telescope observations were taken in 2013 using the EMIR330 receiver and the FFTS backend in the wide mode that covers a 16 GHz instantaneous bandwidth per polarization at a channel spacing of 195 kHz. They are part of a complete millimeter line survey toward the Orion Bar dissociation front (Cuadrado et al. 2014) and include specific deep integration searches for SH^+ $N_J = 1_0-0_1$ lines. The target position is at $\alpha_{2000} = 05^h35^m20.8^s$, $\delta_{2000} = -05°25'17.0''$, close to the so-called CO^+ peak (Stoerzer et al. 1995). The observing procedure was position switching (PSW) with the reference position located at a $(-600'', 0'')$ offset to avoid the extended molecular emission from the Orion Molecular Cloud. The antenna temperature, T_A^*, was converted to the main beam temperature, T_{MB}, using an antenna efficiency of 42 %. At this frequency, the IRAM 30 m telescope provides an angular resolution of 7″. Figure 1 (top panel) shows the resulting spectrum between 345.8 GHz and 345.9 GHz after baseline subtraction. The integration time was 2 h, and the rms noise was ~30 mK per channel. The angular resolution and sensitivity of these observations are a factor of ~2.5 better than those of Leurini et al. (2006). Atmospheric calibration of the IRAM 30 m data was carried out with the ATM program (Cernicharo 1985, IRAM internal report; Pardo et al. 2001).

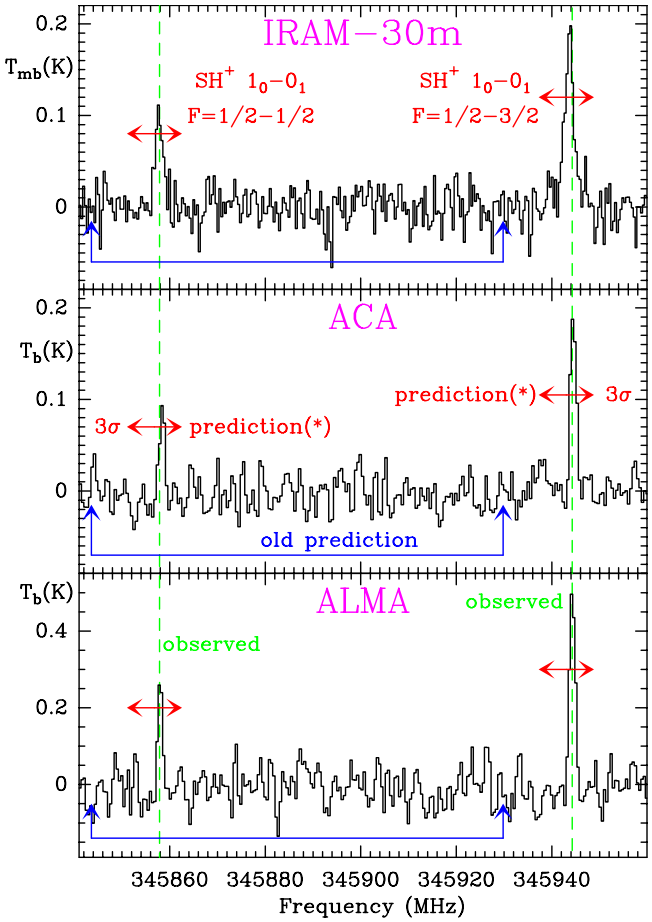

Fig. 1. From *top to bottom*: IRAM 30 m, ACA, and ALMA spectra toward the Orion Bar between 345.8 GHz and 345.9 GHz. Blue arrows show the predicted frequencies of the SH^+, $N_J = 1_0-0_1$, $F = 1/2-1/2$ and $F = 1/2-3/2$ lines before this work (based on experiments by Savage et al. 2004). Red arrows (prediction*) show the expected line frequencies for a Hamiltonian fit that excludes the 345 929.8 MHz line observed by Savage et al. (2004) and attributed to SH^+; see Sect. 4.

2.2. Interferometric ALMA and ACA observations

Atacama Large Millimeter Array (ALMA) observations of the Orion Bar were carried out in 2013 and 2014 during ALMA *Cycle 1* observations. They belong to the 2012.1.00352.S project "The fundamental structure of molecular cloud edges: from clumps to photoevaporation" (P.I.: Goicoechea). They consist of mosaicking observations covering a ~40″ × 40″ field centered at $\alpha_{2000} = 05^h35^m20.6^s$, $\delta_{2000} = -05°25'20.0''$.

The ALMA array observations used twenty-seven 12 m antennas. The field of view was observed as a mosaic of 27 Nyquist-sampled pointings in the C32-2 configuration, providing a typical resolution of ~1″. Observations were carried out with the band 7 receiver near 346 GHz using the ALMA correlator backend at a spectral resolution of 488.3 kHz (~0.4 km s^{-1}) over a total bandwidth of 937.5 MHz. Atacama Compact Array (ACA) is used to complement ALMA observations of extended sources by producing short-spacing visibilities filtered out by the ALMA array. At the time of observations, the ACA array used nine 7 m antennas. The ACA mosaic contained ten pointings Nyquist-sampled fields and provided a typical resolution

of ∼3.6″. The total observing time was about 6.5 h and 2.2 h for ACA and ALMA observations respectively. The data were calibrated within the CASA software package using the standard algorithms. The calibrated uv tables were then exported to GILDAS[1], where the data were deconvolved using the Högbom CLEAN algorithm. All technical details on the data reduction and the complete data set will be presented elsewhere. For the purpose of this work (showing the 345.8−345.9 GHz window observed by different instrumentation) we only deconvolved the ACA and ALMA visibilities separately.

3. Observational results

Figure 1 shows, from top to bottom, the IRAM 30 m, ACA, and ALMA spectra toward the Orion Bar dissociation front; we note that ACA and ALMA spectra are averaged over the same region of the dissociation front. The abscissa axis represents the rest frequency (in MHz) using a local standard of rest velocity (v_{LSR}) of 10.50 km s^{-1}. We derived this v_{LSR} value from the accurately known HCO^+ $J = 4-3$ line frequency[2] observed in the same region of the dissociation front. It agrees, within ∼0.2 km s^{-1}, with typical velocity centroids of other reactive molecular ions observed with single-dish telescopes toward the Orion Bar (see, e.g., Fuente et al. 2003; Leurini et al. 2006; Nagy et al. 2013).

We expected to detect the SH^+ $F = 1/2-1/2$ and $F = 1/2-3/2$ HFS lines of the $N_J = 1_0-0_1$ FS component near 346 GHz on the basis of the previous *Herschel*/HIFI detection of the higher energy SH^+ $N_J = 1_2-0_1$ lines at ∼526 GHz toward the Orion Bar (Nagy et al. 2013). Blue arrows in Fig. 1 show the absence of emission at frequencies derived from previous laboratory data of Savage et al. (2004) for all three telescopes. Our spectra, however, show two emission lines shifted by ∼15 MHz (∼13 km s^{-1}) to higher frequencies with respect to the frequencies indicated by blue arrows, which could not be assigned to other carriers in the MADEX, CDMS (Müller et al. 2001, 2005), and JPL (Pickett et al. 1998) spectroscopic catalogs. Table A.1 shows results from Gaussian fits to the two lines, which were detected with up to 12σ and 7σ significance levels. Averaging the three observations, we obtain 345 944.35 MHz and 345 858.27 MHz for the two lines. Given the complex gas kinematics in Orion, implying an uncertainty in v_{LSR}, we adopted a 1σ systematic uncertainty of 0.2 MHz for the rest frequency determination. We note that the line near 345.9 GHz is only ∼61 MHz (∼53 km s^{-1}) above the CO $J = 3-2$ line frequency.

4. New SH^+ spectroscopic parameters

The two unpaired electrons ($S = 1$) of sulfanylium lead to a $^3\Sigma^-$ electronic ground state which causes all rotational levels N to be split into three with $J = N, N \pm 1$, except for the $N = 0$ level for which only $J = 1$ exists. The lowest order FS parameters are λ and γ which describe the (electron) spin-spin coupling and the (electron) spin-rotation coupling. Rotational (or centrifugal distortion) and vibrational corrections, the latter for excited vibrational states, may appear in the Hamiltonian. The proton magnetic moment ($I_H = 1/2$) splits every FS level into two HFS levels. The main HFS parameters here are b_F and c, the scalar and tensorial electron spin-nuclear spin coupling parameters.

The selection rules $\Delta F = 0, \pm 1$ hold strictly. The spin-conserving transitions ($\Delta F = \Delta J = \Delta N$) are the strongest ones at higher quantum numbers. Other transitions have non-negligible intensities, in particular at low-N. The $N = 1-0$ ground state rotational transition is split into three FS components $J = 0-1$, $2-1$, and $1-1$ near 346, 526, and 683 GHz, respectively, which are split further into 2, 3, and 4 HFS components. An energy level diagram is shown, e.g., in Menten et al. (2011).

The rotation-vibration spectrum of SH^+ was recorded up to $v = 2-1$ (Brown et al. 1986) and $v = 4-3$ (Civiš et al. 1989). Hovde & Saykally (1987) investigated the rotational spectrum of SH^+ in its ground and first excited vibrational state between 0.51 THz and 1.62 THz by laser magnetic resonance (LMR). More recently, Savage et al. (2004) employed source- and velocity-modulation to determine accurate rest frequencies of all three HFS components near 526 GHz of the $N = 1-0$ transition of SH^+ as well as one of two HFS components near 346 GHz. In each of these four studies, spectroscopic parameters were determined only from their own data. In contrast, Brown & Müller (2009) used the field-dependent (Hovde & Saykally 1987) and field-free (Savage et al. 2004) rotational data as well as the rovibrational data of the fundamental ($v = 1-0$) band (Brown et al. 1986; Civiš et al. 1989) to determine ground state spectroscopic parameters as well as vibrational corrections if they were needed. One of the present authors (HSPM) used a slightly different approach to create an entry for the CDMS catalog because the SPFIT program (Pickett 1991) does not permit the use of field-dependent data. The LMR transition frequencies extrapolated to zero field by Brown & Müller (2009) were fit together with the field-free rotational data (Savage et al. 2004) and all of the rovibrational data (Brown et al. 1986; Civiš et al. 1989) to determine Dunham-type parameters $P_{i,j}$ for SH^+, with i and j indicating vibrational and rotational corrections, respectively.

Savage et al. (2004) observed all three HFS components of the $N_J = 1_2-0_1$ transition of sulfanylium (around 526.1 GHz) between 0.2 MHz and 0.5 MHz higher than calculated from the parameters of the LMR study (Hovde & Saykally 1987); the deviations are well within the uncertainties of ∼1.6 MHz from that study. These rest frequencies improve the accuracies of the major HFS parameters b_F and c, as well as the origin of the FS component, which depends on several rotational and fine structure parameters. The $F = 1/2-3/2$ HFS component was found by Savage et al. (2004) only 1.23 MHz higher than calculated from parameters in Hovde & Saykally (1987), well within the uncertainty of ∼18 MHz. The uncertainty is much larger because this FS component was not accessed in the LMR study. The associated $F = 1/2-1/2$ HFS component, weaker by a factor of two, was not detected despite significant signal averaging. Its frequency, ∼86 MHz lower than the $F = 1/2-3/2$ HFS component, is well constrained by the frequency of this HFS component and from the data near 526.1 GHz.

As outlined in Sect. 3, no emission lines were detected in the Orion Bar at the frequencies expected from Savage et al. (2004). However, the two emission lines, each observed ∼15 MHz higher, had the expected 1:2 intensity ratio and spacing required to assign them to the $N_J = 1_2-0_1$ FS component. In order to test the feasibility of these assignments, we omitted the laboratory transition frequency near 346 GHz from the data set which was used to create the CDMS catalog entry. Interestingly, the rms error of the fit improved significantly from 0.898 to 0.826. More importantly, the two HFS components were now predicted at 345 856.8 MHz and at 345 943.0 MHz, very close to our observed emission lines (Fig. 1) and each with predicted 1σ uncertainties of 3.9 MHz. These uncertainties are

[1] See http://www.iram.fr/IRAMFR/GILDAS

[2] We used $\nu(HCO^+4-3) = 356\,734.2244\,(9)$ MHz. All publicly available rotational lines up to $J = 17$ and with uncertainties below 50 kHz (Tinti et al. 2007; Buffa et al. 2006; Hirao et al. 2008; Cazzoli et al. 2012) were used to compute HCO^+ line frequencies with MADEX (Cernicharo 2012). The residual of the fit is 39 kHz.

Table 1. Spectroscopic parameters[a] (MHz, cm^{-1}) of sulfanylium, SH^+.

Parameter	Value
Y_{10}[b]	2 547.4948 (104)
Y_{20}[b]	−49.4293 (90)
Y_{30}[b]	0.2097 (30)
$Y_{40} \times 10^3$[b]	−16.01 (34)
Y_{01}	278 094.99 (36)
Y_{11}	−8577.33 (85)
Y_{21}	16.15 (32)
Y_{02}	−14.7380 (76)
$Y_{12} \times 10^3$	122.9 (27)
$Y_{03} \times 10^3$	0.46[c]
λ_{00}	171 488.3 (58)
λ_{10}	−471.8 (146)
λ_{20}	−79.1 (67)
λ_{01}	−1.13 (24)
γ_{00}	−5036.29 (91)
γ_{10}	116.4 (20)
γ_{20}	3.52 (64)
γ_{01}	0.432 (35)
$b_{F,0}(^1H)$	−56.884 (81)
$b_{F,1}(^1H) - b_{F,0}(^1H)$	−3.46 (79)
$c(^1H)$	33.60 (67)

Notes. [(a)] Numbers in parentheses are one standard deviation in units of the least significant digits. [(b)] In units of cm^{-1}. [(c)] Kept fixed to the value derived by Brown & Müller (2009).

considerably smaller than those from Hovde & Saykally (1987), mainly because of the extensive rovibrational transition frequencies used in the present fit and because of the remaining data from Savage et al. (2004). Hence, we used averages over the three independent observations given in Sect. 3 to redetermine the SH^+ spectroscopic parameters. The resulting parameters are given in Table 1. The rms error of this fit is 0.820, demonstrating that our transition frequencies are more compatible with the remainder of the laboratory data than the single frequency near 346 GHz determined by Savage et al. (2004). Updated predictions of the rotational spectrum of SH^+ will be available in the CDMS catalog[3]. Data up to 1 THz are given in Table A.2.

Errors in rest frequencies determined in the laboratory or through astronomical observations are known to occur especially in sparse data sets. Recent error correction of data pertaining to astrophysically important hydrides include the correction of the fundamental transition of H_2D^+ (Asvany et al. 2008) and of the fundamental transitions of CH^+ isotopologues (Amano 2010).

The changes in spectroscopic parameters are small for the most part and occur predominantly in rotational and FS parameters. The most significant changes of 3σ occur in $Y_{01} \approx B_e$ and $Y_{02} \approx -D_e$. The largest change in magnitude occurs in λ_{00}, but corresponds only to $\sim 1\sigma$. The strong, spin-conserving transitions are only slightly affected at lower frequencies. In addition, the transitions of the $N_J = 1_1 - 0_1$ FS component (~683 GHz) are now predicted 2 MHz lower than in the first SH^+ CDMS catalog entry. Changes from the predictions by Brown & Müller (2009) are a bit more complex, but deviate on average by ~2 MHz. Larger deviations of several megahertz may occur for transitions with flip of the electron spin (e.g., at ~893 GHz) or at higher frequencies.

The 345 929.8 MHz line observed in the laboratory, and attributed to SH^+, $N_J = 1_0 - 0_1$, $F = 1/2 - 3/2$ by Savage et al. (2004), is not detected at the sensitivity limit of our observations. Here we demonstrate that the 345 929.8 MHz line is not SH^+, and we improve the SH^+ spectroscopic parameters with the detection of the 345 944 and 345 858 MHz lines, which arise from the edge of the Orion Bar, consistent with the expected SH^+ formation route in PDRs, the reaction of S^+ with vibrationally excited H_2 (e.g., Nagy et al. 2013; Zanchet et al. 2013). Nevertheless, it may still be useful to reinvestigate the $N = 1 - 0$ transition of SH^+ in the laboratory using methods such as those by Savage et al. (2004); Asvany et al. (2008); Amano (2010); Brünken et al. (2014), in particular in combination with a study of $^{34}SH^+$.

Acknowledgements. We thank the Spanish MINECO for funding support under grants CSD2009-00038, AYA2009-07304, and AYA2012-32032. We thank the European Research Council for funding support under ERC-2013-Syg 610256-NANOCOSMOS. H.S.P.M. is supported by the German Bundesministerium für Bildung und Forschung (BMBF) via the ALMA Regional Center (ARC) Node project 5A11PK3 for maintanance and upgrade of the CDMS. J.R.G. thanks the Observatoire de Paris/ENS and IRAM (Grenoble) where part of this work was carried out. S.C. was supported by a FPI-INTA grant.

References

Abel, N. P., Federman, S. R., & Stancil, P. C. 2008, ApJ, 675, L81
Amano, T. 2010, ApJ, 716, L1
Asvany, O., Ricken, O., Müller, H. S. P., et al. 2008, Phys. Rev. Lett., 100, 233004
Barlow, M. J., Swinyard, B. M., Owen, P. J., et al. 2013, Science, 342, 1343
Benz, A. O., Bruderer, S., van Dishoeck, E. F., et al. 2010, A&A, 521, L35
Brown, J. M., & Müller, H. S. P. 2009, J. Mol. Spectrosc., 255, 68
Brown, P. R., Davies, P. B., & Johnson, S. A. 1986, Chem. Phys. Lett., 132, 582
Brünken, S., Kluge, L., Stoffels, A., Asvany, O., & Schlemmer, S. 2014, ApJ, 783, L4
Buffa, G., Dore, L., Tinti, F., & Meuwly, M. 2006, Chem. Phys. Chem., 7, 176
Cazzoli, G., Cludi, L., Buffa, G., & Puzzarini, C. 2012, ApJS, 203, 11
Cernicharo, J. 2012, in Proc. of the European Conference on Laboratory Astrophysics, eds. C. Stehleé, C. Joblin, & L. d'Hendecourt, Eur. Astron. Soc. Publ. Ser., 4
Civiš, S., Blom, C. E., & Jensen, P. 1989, J. Mol. Spectrosc., 138, 69
Cuadrado, S., Goicoechea, J. R., Pilleri, P. et al. 2014, A&A, submitted
Etxaluze, M., Goicoechea, J. R., Cernicharo, J., et al. 2013, A&A, 556, A137
Fuente, A., Rodrıguez-Franco, A., Garcıa-Burillo, S., Martın-Pintado, J., & Black, J. H. 2003, A&A, 406, 899
Godard, B., Falgarone, E., Gerin, M., et al. 2012, A&A, 540, A87
Goicoechea, J. R., Joblin, C., Contursi, A., et al. 2011, A&A, 530, L16
Hirao, T., Yu, S., & Amano, T. 2008, J. Mol. Spectrosc., 248, 26
Hovde, D. C., & Saykally, R. J. 1987, J. Chem. Phys., 87, 4332
Leurini, S., Rolffs, R., Thorwirth, S., et al. 2006, A&A, 454, L47
Lis, D. C., & Schilke, P. 2003, ApJ, 597, L145
Menten, K. M., Wyrowski, F., Belloche, A., et al. 2011, A&A, 525, A77
Müller, H. S. P., Thorwirth, S., Roth, D. A., & Winnewisser, G. 2001, A&A, 370, L49
Müller, H. S. P., Schlöder, F., Stutzki, J., & Winnewisser, G. 2005, J. Mol. Struct., 742, 215
Nagy, Z., van der Tak, F. F. S., Ossenkopf, V., et al. 2013, A&A, 550, A96
Neufeld, D. A., Falgarone, E., Gerin, M., et al. 2012, A&A, 542, L6
Pardo, J. R., Cernicharo, J., & Serabyn, E. 2001, IEEE Trans. Antennas Propag., 49, 1683
Pickett, H. M. 1991, J. Mol. Spectrosc., 148, 371
Pickett, H. M., Poynter, R. L., Cohen, E. A., et al. 1998, JQSRT, 60, 883
Savage, C., Apponi, A. J., & Ziurys, L. M. 2004, ApJ, 608, L73
Schilke, P., Neufeld, D. A., Müller, H. S. P., et al. 2014, A&A, 566, A29
Stäuber, P., Benz, A. O., Jørgensen, J. K., et al. 2007, A&A, 466, 977
Stoerzer, H., Stutzki, J., & Sternberg, A. 1995, A&A, 296, L9
Tinti, F., Bizzocchi, L., Degli Esposti, C., & Dore, L. 2007, ApJ, 669, L113
Zanchet, A., Agúndez, M., Herrero, V. J., Aguado, A., & Roncero, O. 2013, AJ, 146, 125

[3] See http://www.astro.uni-koeln.de/cdms/catalog

Appendix A: Complementary tables

Table A.1. Gaussian fits to the $F = 0.5{-}1.5$ and $0.5{-}0.5$ lines of the $N_J = 1_0{-}0_1$ FS component of SH^+ observed with three different telescopes toward the Orion Bar (for v_{LSR}=10.50 km s^{-1}).

Telescope	Line	Rest frequency (MHz)	$\int T_{mb}\,dv$ (mK km s^{-1})	Line width (km s^{-1})	Signal-to-noise
IRAM 30 m					
	1.5–0.5	345 944.22 (20)	383 (30)	1.95 (19)	~10
	0.5–0.5	345 858.38 (20)	185 (31)	1.68 (32)	~5
ACA					
	1.5–0.5	345 944.55 (20)	260 (20)	1.23 (10)	~12
	0.5–0.5	345 858.42 (20)	114 (25)	1.10 (26)	~6
ALMA					
	1.5–0.5	345 944.29 (20)	668 (51)	1.20 (10)	~12
	0.5–0.5	345 858.00 (20)	295 (58)	0.92 (20)	~7

Notes. Parentheses show the Gaussian fit uncertainties (in units of the least significant digits). For the fitted frequencies, we adopt an overall 1σ uncertainty of 0.2 MHz (~0.2 km s^{-1}). This should be considered as a systematic uncertainty due to uncertainties in v_{LSR} (see text). IRAM 30 m spectrum smoothed to ~0.4 km s^{-1}, similar to ALMA and ACA; signal-to-noise determined on the peaks and refering to ~0.4 km s^{-1} resolution for IRAM 30 m and to the native spectral resolution for ALMA and ACA.

Table A.2. Quantum numbers, frequencies (MHz), uncertainties unc. (MHz), Einstein A values (10^{-4} s^{-1}), upper g_{up} and lower g_{lo} state degeneracies, and upper E_{up} and lower E_{lo} state energies (cm^{-1}) of sulfanylium, SH^+, below 1 THz.

$N' - N''$	$J' - J''$	$F' - F''$	Frequency	unc.	A	g_{up}	g_{lo}	E_{up}	E_{lo}
1–0	0–1	0.5–0.5	345 858.1957	0.1494	1.15	2	2	11.5395	0.0029
1–0	0–1	0.5–1.5	345 944.4205	0.1496	2.30	2	4	11.5395	0.0000
1–0	2–1	1.5–0.5	526 038.7348	0.0699	8.00	4	2	17.5496	0.0029
1–0	2–1	2.5–1.5	526 047.9440	0.0714	9.59	6	4	17.5471	0.0000
1–0	2–1	1.5–1.5	526 124.9597	0.0723	1.60	4	4	17.5496	0.0000
1–0	1–1	1.5–0.5	683 334.0618	0.5139	2.90	4	2	22.7964	0.0029
1–0	1–1	0.5–0.5	683 359.9250	0.4790	11.59	2	2	22.7973	0.0029
1–0	1–1	1.5–1.5	683 420.2867	0.4972	14.48	4	4	22.7964	0.0000
1–0	1–1	0.5–1.5	683 446.1499	0.4942	5.79	2	4	22.7973	0.0000
2–1	1–1	0.5–0.5	893 065.8800	0.9514	19.77	2	2	52.5868	22.7973
2–1	1–1	0.5–1.5	893 091.7433	0.9763	9.89	2	4	52.5868	22.7964
2–1	1–1	1.5–0.5	893 126.2353	1.0505	4.94	4	2	52.5888	22.7973
2–1	1–1	1.5–1.5	893 152.0985	0.9475	24.73	4	4	52.5888	22.7964